FULL PAPER

Dalton
www.rsc.org/dalton

Bicyclic phosphines as ligands for cobalt-catalysed hydroformylation †

Chantelle Crause,* Linette Bennie, Llewellyn Damoense, Catherine L. Dwyer, Cronje Grove, Neil Grimmer, Werner Janse van Rensburg, Megan M. Kirk, Konrad M. Mokheseng, Stefanus Otto and Petrus J. Steynberg

Sasol Technology R&D, P.O. Box 1, Sasolburg 1947, South Africa.
E-mail: chantelle.crause@sasol.com

Received 29th October 2002, Accepted 19th December 2002
First published as an Advance Article on the web 23rd April 2003

A range of tertiary phosphine ligands derived from (*R*)-(+)-limonene was studied by HP-^{31}P NMR, HP-IR, batch autoclave reactions and molecular modelling during the hydroformylation of 1-dodecene using a cobalt catalyst system and a metal : ligand ratio of 1 : 2. The phosphorus atom was incorporated in a limonene bicycle where the third substituent was systematically varied, Lim-R (R = $(CH_2)_{17}CH_3$, $(CH_2)_9CH_3$, $(CH_2)_4CH_3$, $(CH_2)_3CH_3$, $(CH_2)_3C_6H_5$, $(CH_2)_3CN$, $(CH_2)_3OCH_2C_6H_5$, $(CH_2)_2OCH_2CH_3$). The activity and selectivity was, to a large extent, governed by the equilibria between the modified and unmodified cobalt catalytic species in the reaction. Linearity ranged from 54 to 71% with Lim-$(CH_2)_3CN$ yielding the most branched product and Lim-$(CH_2)_4CH_3$ the most linear product. The n : iso ratio (ratio of linear to 2-methyl branched alcohol) also followed the same trend with a ratio of 2.6 for Lim-$(CH_2)_3CN$ and 4.9 for Lim-$(CH_2)_4CH_3$. The rate decreased as the linearity increased with pseudo *k* values of 0.5 to 1.1. Hydrogenation of the alkene varied within a narrow band from 5–6%.

Introduction

Ever since the discovery of cobalt-catalyzed hydroformylation (also known as the oxo process) by Otto Roelen[1] in 1938 its industrial importance has been recognized.[2] In the first two decades since the discovery of the reaction the active catalytic system was based on the unmodified $HCo(CO)_4$ complex derived from either Co(0) or from Co(II) *via* $Co_2(CO)_8$ treatment with a 1 : 1 mixture of CO and H_2 (syngas) at high pressures and temperature. However, high reaction pressures were required to ensure the stability of the active catalyst. In 1968, it was reported[3] that the addition of a tertiary phosphine could stabilise the catalyst to such an extent that reaction pressures below 100 atm were feasible. Although the phosphine modified Co catalyst system is less reactive than the unmodified catalyst, the increased electron density on the metal centre affords a better hydrogenation catalyst which results in the formation of alcohols rather than aldehydes as the primary products. Thus where alcohols are required as the end product, a substantial hydrogenation step is unnecessary. Unfortunately, due to this improved hydrogenation capability some of the olefin feedstock can be lost *via* the competing hydrogenation of the alkenes to the corresponding alkanes. It is believed that the higher selectivity of the modified catalyst towards linear product is a result of the larger steric demand of a tertiary phosphine compared to CO.[4,5] This would influence the orientation of the olefin during insertion into the Co–H bond.

Although hydroformylation is the oldest homogeneous process in use today, research groups worldwide are still actively pursuing improvements to obtain a highly selective catalyst system without sacrificing reaction rate and olefin hydrogenation. It has been observed that an increase in the ratio of phosphine to cobalt decreases the rate of hydroformylation with a concomitant increase in selectivity to linear products.[6,7] These observations were rationalised on the basis of the suggested hydroformylation mechanism for propene in the presence of $Co_2(CO)_6(PBu_3)_2$. The Heck and Breslow mechanism has been generalised and extrapolated to the phosphine-modified system in which the pre-catalytic species is the mono-substituted hydride, $HCo(CO)_3L$. The hydride is formed by splitting of the dimer, $[Co(CO)_3L]_2$ with hydrogen under reaction conditions. The effect of the 'unmodified' $HCo(CO)_4$ and 'modified' $HCo(CO)_3L$ catalytic species was considered (Scheme 1). The higher selectivities observed were attributed to

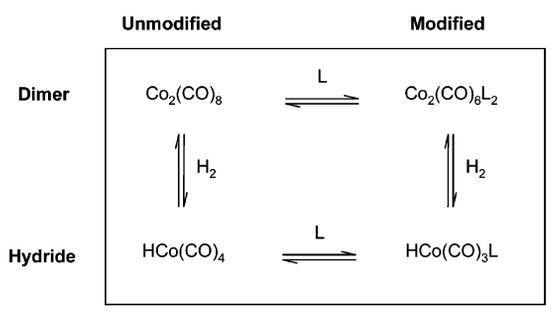

Scheme 1 Reaction scheme and notation.

an increase in the percentage of phosphine substituted hydride complexes with an increase in the free phosphine concentration. Furthermore, the decrease in reaction rate as the concentration of modified species was increased was ascribed to the lower reactivity of the modified species. However, not only ligand concentration influences the ratio of modified to unmodified catalytic species but also the nature of the ligand employed. Simple trialkylphosphines such as tributylphosphine have been widely used as ligands but bulky bicyclic phosphines have been preferred due to reduced volatility and catalyst stability. A particularly favoured tertiary phosphine is 9-eicosyl-9-phosphabicyclononane as disclosed by Shell.[8] In this regard we wish to report our results on a family of (*R*)-(+)-limonene based bicyclic phosphine ligands[9] studied by HP-^{31}P NMR, HP-IR, batch autoclave reactions and molecular modelling during the hydroformylation of 1-dodecene using a cobalt catalyst system (Scheme 2).

Experimental

Chemicals

Toluene (Riedel de Haen) and diethyl ether (Saarchem) were freshly distilled from sodium benzophenone ketyl prior to use.

† Based on the presentation given at Dalton Discussion No. 5, 10–12th April 2003, Noordwijkerhout, The Netherlands.

DOI: 10.1039/b210650g

Table 1 Abbreviations for the Lim-R derivatives investigated and selected physical properties

Abbreviation	R	Bp/°C	δ ^{31}P[a]/ppm	δ O=P ^{31}P/ppm
Lim-H	H	228–233	−72.4; −96.5	36.2; 29.7; 26.4; 21.5
Lim-C_{18}	$(CH_2)_{17}CH_3$	481–486	−44.6; −51.4	50.0; 48.1
Lim-C_{10}	$(CH_2)_9CH_3$	365–370	−44.7; −51.4	48.1; 46.0
Lim-C_5	$(CH_2)_4CH_3$	301–306	−44.2; −50.9	48.3; 46.3
Lim-C_4	$(CH_2)_3CH_3$	280–285	−44.2; −50.8	48.4; 46.4
Lim-APh	$(CH_2)_3C_6H_5$	358–363	−45.2; −51.9	48.3; 46.4
Lim-ACN	$(CH_2)_3CN$	311–316	−45.1; −52.2	47.9; 46.1
Lim-ABE	$(CH_2)_3OCH_2C_6H_5$	391–396	−43.7; −50.4	48.9; 46.8
Lim-EVE	$(CH_2)_2OCH_2CH_3$	297–302	−48.7; −55.1	46.8; 45.5

[a] A downfield chemical shift corresponds to the Lim-4*R* isomer (−45 ppm) whilst an upfield chemical shift corresponds to the Lim-4*S* isomer (−51 ppm).

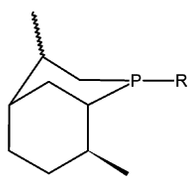

Scheme 2 Tertiary phosphine ligands derived from (*R*)-(+)-limonene. See Table 1 for a definition of R groups.

BuLi (Aldrich, 2.5 M in hexane), 1-bromobutane (Aldrich, 99%), allylbenzene (Aldrich, 98%), allylcyanide (Aldrich, 98%), allyl benzyl ether (Aldrich, 99%), ethyl vinyl ether (Aldrich, 99%), 2,2′-azobisisobutyronitrile, AIBN (Wako), $Co_2(CO)_8$ (Aldrich), $CDCl_3$ (Aldrich), toluene-d_8 (Aldrich), cobalt-(2-ethylhexanoate) (Comar Chemicals), the Lim-H phosphine (Cytec) and syngas (H_2 : CO, 2 : 1, Afrox, 99.98%) were used as received. The C9/C11 paraffin cut (C_8 13, C_9 29, C_{10} 30, C_{11} 28%), and 1-dodecene (>95%) were Fisher Tropsch derived products supplied by Sasol.

Preparation of ligands

The ligands were treated as oxygen sensitive and all manipulations were carried out in clean, dry Schlenk glassware under an argon atmosphere using degassed solvents. Boiling points of the ligands were obtained from SimDist analysis and are reported as a 5 °C boiling range. All ligands were purified by either short-path distillation or Kugelrohr distillation to a purity of >90% (as determined by ^{31}P NMR analysis) before use; the main source of impurities is the corresponding phosphine oxides. Boiling points and ^{31}P NMR chemical shifts in $CDCl_3$ for the ligands are summarised in Table 1. All ligands were synthesised according to one of the following two methods.

Method 1. A toluene solution (50 ml) of AIBN (500 mg) was added over an 8 h period to a solution of Lim-H (10 g; 59 mmol) and the appropriate olefin (>75 mmol) in toluene at 90 °C. After 16 h conversion to the corresponding Lim-R complex was usually complete and the toluene and excess olefin were removed under vacuum. Kugelrohr distillation of the resulting viscous residues gave the ligands as colourless oils in purities of >90%. Isolated yields were in excess of 70% for all ligands prepared in this way.

Method 2. A diethyl ether solution containing Lim-H (10 g; 59 mmol) at −78 °C was treated with BuLi (25.8 ml, 2.5 M, 65 mmol) and the temperature was allowed to reach 0 °C over 20 minutes. The solution was cooled down to −30 °C and 1-bromobutane (8.90 g, 7.0 ml, 65 mmol) was added drop wise over 10 minutes after which time it was left to stir at room temperature for 16 h resulting in complete conversion to the desired product. The reaction was quenched with a degassed aqueous ammonium chloride solution and extracted with anhydrous ether. The combined ether fractions were dried over anhydrous magnesium sulfate and the volatile components were removed under reduced pressure. Kugelrohr distillation gave the Lim-C_4 ligand in a purity of 89% with an isolated yield of 72%.

Molecular modelling

All geometry optimizations were performed with the DMol^3 Density Functional Theory (DFT) code[10] as implemented in the MaterialsStudio™ (version 2.1.5) program package of Accelrys Inc.[11] on SGI and Compaq Alpha workstations. In DMol^3 the wave functions are expanded in terms of accurate numerical basis sets. In this study the double numerical basis set (DNP) containing a p-polarization function for H and d-polarization functions for other atoms was used. The DNP basis set was chosen because it is equivalent in quality and size to the Gaussian 6-31G** split-valence double-zeta plus polarization basis set, generally accepted as the standard basis set in quantum chemistry. The generalized gradient approximation (GGA) functional by Perdew and Wang (PW91)[12] was used for all geometry optimisations. The convergence criteria for these optimisations consisted of threshold values of 2×10^{-5} Ha, 0.00189 Ha Å^{-1} and 0.00529 Å for energy, gradient and displacement convergence, respectively, while a self consistent field (SCF) density convergence threshold value of 1×10^{-6} was specified. All calculated reaction energies were derived from the total electronic energies of the geometries after optimisation.

In the case of Lim-C_{18}, Lim-C_{10}, $HCo(CO)_3$Lim-C_{10} and $HCo(CO)_3$Lim-C_{18} an annealing dynamics protocol, involving 200 steps of dynamics, a time step of 0.0005 ps, an initial temperature of 200 K, a midcycle temperature of 2000 K and a temperature increment of 200 K, was followed to yield the most stable conformers. The dynamics was performed with the anneal molecular dynamics functionality incorporated in the Accelrys Cerius^2 (version 4.6) program suite,[11] using the universal force field (UFF).[13] The trigonal bipyrimidal arrangement of the cobalt metal centre was constrained during the MD runs due to the lack of appropriate force field parameters for Co and the said geometry.

After each MD run the ten most stable conformers were subjected to a full geometry optimisation with the semi empirical PM3 method[14] as incorporated in the Spartan '02 for Unix program package available from Wavefunction.[15] The conformer with lowest SE/PM3 predicted total electronic energy was used for consequent DFT geometry optimisation as described above. This procedure was followed to ensure that global minima structures for both ligand and complex structures were obtained. For the C_{10} and C_{18} structures different global minima conformations for the alkyl chains for the ligand and the respective complex were found. No additional conformations for ligands and complexes were optimized at the DFT level, because for the purpose of this comparative study only the lowest energy structures are important.

IR measurements

All infrared spectra were recorded with a Nexus 670 FT-IR spectrometer from Nicolet. The design, construction and mode of operation of the high pressure infrared cell have been described earlier.[16] All spectra were collected using Happ-Genzel apodization.

The samples were prepared by dissolving $Co_2(CO)_8$ and the phosphine ligand under investigation under an argon atmosphere in a C9/C11 paraffin mixture to give a final cobalt concentration of 1000 ppm, and a cobalt to phosphine ratio of 1 : 2. The solutions were pressurized in the high pressure IR cell with syngas at room temperature to approximately 56.5 bar. The solutions were heated to 170 °C with constant stirring to give a final calculated pressure of approximately 85 bar syngas pressure.

High pressure NMR measurements

All ^{31}P NMR spectra were recorded using a Waltz 16 ^{1}H decoupling sequence on either a Varian Unity Inova 400 MHz or a 500 MHz Bruker Avance NMR spectrometer operating at 161.905 and 202.466 MHz respectively and were calibrated relative to an external sample of H_3PO_4 at 0 ppm. The high pressure experiments were performed in a 10 mm high pressure Roe cell[17] and the spectra were recorded without spinning. Spectra were recorded at 30, 90, 120, 150 (immediately), 150 (1 hour), 150 (2 hours), 120 and 30 °C. For each spectrum on the Varian instrument 128 transients were collected using a 45° pulse and a 2 second delay time. On the Bruker instrument spectra containing 128 transients were recorded using a 30° pulse and a 2 second delay time.

The samples were prepared by weighing $Co_2(Co)_8$ (20 mg) into an argon-filled sample tube and dissolving it in toluene (1.5 ml). The phosphine ligand (2.5 molar equivalents to cobalt) was dissolved in toluene-d_8 (0.5 ml) and transferred under argon to the sample tube. The HP-NMR cell was flushed with argon, and the reaction solution was transferred *via* syringe into the cell. The cell was closed and purged by pressurising to 60 bar with syngas and releasing pressure several times. Once pressurised to the desired operating pressure (60 bar), the cell was left overnight (at least 15 hours) to allow proper gas dissolution before acquisition of spectra. Since the titanium head of the Roe high pressure NMR cell is glued to the single crystal sapphire cell the solution cannot be shaken to aid in the gas diffusion for fear of damaging the glued section with organic solvents.

Kinetic measurements

The C9/C11 paraffin mixture used as solvent and 1-dodecene were degassed with argon prior to use. Cobaltbis(2-ethylhexanoate) was purchased as a viscous 12% (Co m/m) solution in alkanes and a 10000 ppm stock solution was prepared using C9/C11 paraffin. The batch autoclave reactions were performed in a 300 ml Parr model 4560 stainless steel autoclave, electrically heated, with a magnetic drive stirrer and an internal cooling coil connected to a silicone oil bath (Lauda Integra T1200) at 35 °C.

All experimental conditions employed are reported in the text. The autoclave was charged under argon with 1-dodecene, paraffin solvent, cobalt(II) precursor and the phosphine ligand and was subsequently flushed with syngas and stirring at 1000 min^{-1} was commenced. After heating to the desired reaction temperature (temperature control within 2 °C) the autoclave was pressurised to the desired pressure with syngas from a buffer vessel. The pressure drop in this buffer vessel was monitored to determine the syngas consumption. After 12 hours the autoclave was cooled to 30 °C, the vessel was depressurised and samples were removed for GC analysis.

The analysis of the reaction products at the end of the run was performed by gas chromatography using an Agilent 6890 series GC system equipped with a Hewlett Packard Pona column (50 m × 0.2 mm × 0.5 μm) and FID detector. Temperature program: 100 °C (hold 10 min), 250 °C (2 °C min^{-1}), 250 °C (5 min), 300 °C (10 °C min^{-1}), 300 °C (5 min). Carrier gas flow: constant at 0.7 ml min^{-1}.

Results and discussion

Preparation of ligands

Synthesis of the secondary alkyl phosphine, 4,8-dimethyl-2-phosphabicylo[3.3.1]nonane (Lim-H) by the radical addition of PH_3 to (*R*)-(+)-limonene[18] results in two diastereomers which arise due to the orientation of the 4-methyl groups in either the axial or equatorial position as evident from ^{31}P NMR and GC-MS analysis. The third functional group was introduced on the P centre either by radical addition of an appropriate olefin, or by deprotonation of the secondary phosphine (Lim-H) with BuLi followed by treatment with an alkyl- or aryl-halide as shown in eqns. (1) and (2) respectively:

$$\text{Lim-H} + CH_2{=}CH\text{-R} \xrightarrow{\text{AIBN}} \text{Lim-}CH_2CH_2\text{-R} \qquad (1)$$

$$\text{Lim-H} + \text{Bu-Li} \rightarrow \text{Lim-Li} \xrightarrow{\text{Br-Bu}} \text{Lim-Bu} \qquad (2)$$

All ligands were obtained in >70% yield and were conveniently purified by Kugelrohr distillation to >90% purity. The ^{31}P NMR spectra of all ligands were very characteristic clearly showing the resonances for the two isomers in the −40 to −55 ppm region, see Table 1.

Molecular modelling

When one equivalent of Lim-C_{18} is added to $Co_2(CO)_8$ it is observed from ^{31}P NMR spectroscopy that all the ligand coordinates to the cobalt. However, if an excess of Lim-C_{18} is added it is observed that one isomer coordinates preferentially to the other. Theoretical ^{31}P NMR shielding tensors were calculated using the gauge-including atomic orbital (GIAO) method[19] incorporated in the Gaussian 98[20] *ab-initio* program. Equilibrium geometries were obtained with Accelrys software, *vida supra*. Isotropic shieldings of 383.4 and 407.3 ppm for the Lim-4*R*-C_{18} and Lim-4*S*-C_{18} respectively can be converted to chemical shifts using a reported absolute chemical shielding value for 85% aqueous H_3PO_4,[21] σ = 328.4 ppm (*i.e.* 328.4 − 383.4 = −55.0 ppm for Lim-4*R*-C_{18} and 328.4 − 407.3 = −78.9 ppm for Lim-4*S*-C_{18}). The absolute difference between the calculated chemical shifts (23.9 ppm) is somewhat larger than the experimentally obtained absolute difference of 6.8 ppm. Consideration of the relatively large detectable NMR range (roughly 1000 ppm) for ^{31}P, makes the accuracy acceptable. ^{31}P NMR experiments have indicated that the ligand corresponding to the downfield chemical shift reacts in preference with the metal precursor. The theoretical ^{31}P NMR calculations presented here indicate that the downfield ^{31}P NMR shift corresponds to the Lim-4*R*-C_{18} isomer. The calculated reaction energies for the coordination of Lim-4*R*-C_2, Lim-4*S*-C_2, Lim-4*R*-C_{18} and Lim-4*S*-C_{18} to $HCo(CO)_4$ are summarised in Table 2.

The results in Table 2 show that coordination of the Lim-4*R* isomers proceed in preference to the 4*S* isomers as is evident from the higher calculated exothermicities for coupling of the 4*R* isomers. These results complement the experimental observation of preferred coupling of one Lim isomer when excess ligand to metal molar fractions are used. In collaboration with this group, Cole-Hamilton[22] investigated the cobalt dimers of the two Lim-C_{18} isomers when excess ligand to metal molar fractions are used. These isomers were isolated, characterised and the hydroformylation reactivity studied.

Table 2 Calculated reaction energies for coordination of Lim diastereoisomers

Ligand	Energy/kcal mol^{-1}
Lim-4*R*-C_2	−0.74
Lim-4*S*-C_2	−0.43
Lim-4*R*-C_{18}	−0.82
Lim-4*S*-C_{18}	2.24

Table 3 Modified : unmodified (IR), %hydride formation under catalyst pre-forming and DFT (GGA/PW91) ligand coordination reaction energies

Ligand	M : U (IR)	%Hydride (NMR)	MM ΔE/kcal mol^{-1}
Lim-C_{18}	4.2	27	−0.82
Lim-C_{10}	11	33	1.17
Lim-C_5	20	33	1.20
Lim-C_4	25	—	1.27
Lim-APh	3.7	28	2.37
Lim-ACN	1.9	—	3.04
Lim-ABE	5.3	30	1.70
Lim-EVE	3.8	22	1.44

The coordination strength of the Lim-R phosphine ligands was estimated by calculating the reaction energy of the following equilibrium reaction for each ligand as shown in eqn. (3).

(3)

$$\Delta E(\text{reaction}) = E[HCo(CO)_3\text{Ligand}] + E[CO] - E[HCo(CO)_4] - E[\text{Ligand}]$$

For all structures considered, full geometry optimisations, with no atom constraints, were performed. The calculated reaction energies thus include stabilisation due to both electronic relaxation and deformation of the ligand upon complexation.

The calculated reaction energies for ligand coordination to $HCo(CO)_4$ are summarised in Table 3. From the results summarised in Table 3 it is evident that the coordination of the ligands is slightly endothermic. The magnitude of this endothermicity of ligand coordination may be compared to the ratio of unmodified *versus* modified catalytic species present in the experimental investigations. The higher the calculated endothermicity of ligand coordination to $HCo(CO)_4$ the higher the unmodified : modified ratio should be. The theoretical results summarised in Table 3 suggest that the Lim-ACN ligand will form the lowest proportion of modified catalyst whilst Lim-C_{10} will form the highest proportion when the results for reaction energies in the range 1.17 to 3.04 kcal mol^{-1} are compared. These theoretical results follow the same general trend for modified and unmodified catalysis that was determined from the experimental IR studies on these ligand systems, see Fig. 1. The exothermic reaction energy calculated for Lim-C_{18} (−0.82 kcal mol^{-1}) does not follow the trend calculated for the other ligands. This phenomenon may be attributed to favourable folding of the C_{18} alkyl fragments of both the complex and free ligand in the calculations. It is believed that errors in the calculated reaction energies for different conformations of the Lim-C_{18} model will be larger than the narrow range of calculated reaction energies obtained for the other models. Therefore, the result obtained for Lim-C_{18} was not used for direct comparison with the other models. In order to ascertain the steric influence of the R groups, attached to P, the reaction energy for sterically less demanding Lim-R (R = Me; H) was also calculated. From this result it is predicted that Lim-Me will coordinate to $HCoCO_4$ with a reaction energy of −0.46 kcal mol^{-1}, effectively illustrating an increase in coordination strength relative to the sterically more demanding ligands listed in Table 3. The

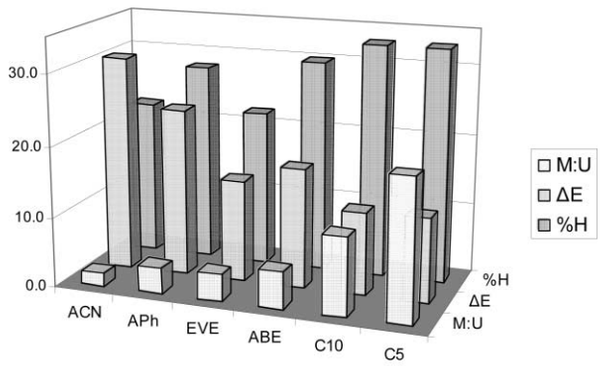

Fig. 1 Comparison of HP-IR, HP-NMR and modelling trends.

reaction energy for Lim-H coordination was calculated as 1.51 kcal mol^{-1}, which shows that electronic changes upon changing from R = Me to R = H will dominate the coordination strength of the ligand despite the more favourable steric nature of Lim-H compared to Lim-Me. Both Lim-H and Lim-Me will be included in future experimental studies. These theoretical results show that caution needs to be taken when steric effects are considered for ligand coordination, because both steric and electronic effects are combined in the calculated reaction energies. This is especially true for the narrow energy range found for ligand coordination in this study.

High pressure spectroscopic studies

High-pressure/high temperature infrared and NMR measurements were used to study the pre-catalytic equilibria under standard hydroformylation reaction conditions. These techniques were used in conjunction to account for all the species present during the catalytic pre-forming cycle; since the carbonyl stretching frequency is very diagnostic and isolated from interference by other peaks it is a most suitable handle for study by IR spectroscopic techniques whilst NMR measurements gave information concerning the phosphorus containing species in solution. It was anticipated that information regarding the species present during the pre-forming cycle could be used to predict catalytic behaviour.

(a) IR measurements. The peak assignments to the different cobalt species were based on literature values,[23] a typical IR spectrum is depicted in Fig. 2. IR characterization of the different Co carbonyl species in solution is given in Table 4. For the modified dimers the stretching frequency of the main absorption of the carbonyl groups varies only from 1950 to 1952 cm^{-1}. A similar narrow range is observed for the modified hydride carbonyl groups.

Fourier deconvolution was performed to separate the peaks at 2029 ($CoH(CO)_4$) and 2021 cm^{-1} ($Co_2(CO)_7L$). Negative peaks were eliminated by adjusting the bandwidth and

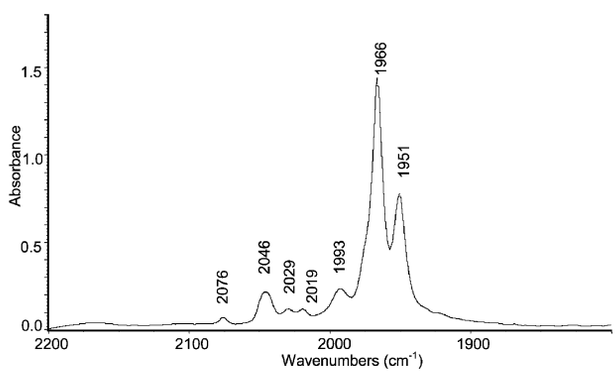

Fig. 2 $Co_2(CO)_8$ + Lim-ABE, Co : L = 1 : 2, 100 °C, 71 bar syngas.

Table 4 IR and ^{31}P NMR characterisation of the species in solution[a]

Ligand	$[Co(CO)_3L]_2$ ν(CO)/cm^{-1}	$[CoH(CO)_3L]$ ν(CO)/cm^{-1}	$[Co(CO)_3L]_2$ δ ^{31}P/ppm	$[CoH(CO)_3L]$ δ ^{31}P/ppm
Unmodified	—	2114 w 2052 m 2029s 1993 vw	—	—
Lim-C_{18}	1966 w 1951 vs 1933 vw	2046 mw 1966 vs	38.1, 40.5	26.5, 27.8
Lim-C_{10}	1969 w 1950 vs 1920 vw	2045 mw 1966 vs	38.2, 40.7	26.8, 27.8
Lim-C_5	1968 w 1952 vs 1932 w	2045 mw 1966 vs 1975 (sh)	38.2, 40.7	26.7, 27.6
Lim-C_4	1966 w 1950 vs 1922 w	2046 mw 1966 vs	38.6, 41.4	26.7, 27.6
Lim-APh	1968 w 1951 vs 1923 w	2045 mw 1966 vs	38.4, 40.4	26.8, 27.5
Lim-ACN	1968 vw 1953 vs 1921 w	2048 mw 1968 vs	38.1, 40.2	26.7, 27.1
Lim-ABE	1969 w 1951 vs 1923 w	2046 mw 1966 vs	39.2, 41.5	27.8, 28.6
Lim-EVE	1969 w 1952 vs 1923 w	2045 mw 1967 vs	39.5, 41.6	28.2, 29.1

[a] Downfield chemical shifts correspond to Lim-4*S* cobalt complexes whilst upfield chemical shifts correspond to Lim-4*R* cobalt complexes.

enhancement. The ratio of the $CoH(CO)_4$ (2029 cm^{-1}) to $CoH(CO)_3L$ (2045 cm^{-1}) peaks were calculated using peak areas. The weaker peak at 2045 cm^{-1} for $CoH(CO)_3L$ was chosen instead of the stronger peak at 1960–70 cm^{-1} due to the overlap of the latter with one of the peaks originating from $Co_2(CO)_6L_2$. Although weak paraffin bands (around 2026 cm^{-1}) exist in the region where $CoH(CO)_4$ absorbs, it is not observed at high temperatures where the path length is fairly small. Peak area ratios for $CoH(CO)_4$ and $CoH(CO)_3L$ are given in Table 3. It should be noted that only peak area ratios are quoted and these do not represent absolute quantification of the species present. Although small variations could be expected it was assumed that, since the phosphine ligands are very similar, the complexes would have very similar molar extinction coefficients. It was found that these ratios corresponded well with other experimental observations and thus can be used, in this specific system, as a fairly accurate indication of the modified : unmodified ratio.

(b) High pressure NMR measurements. *In situ* high-pressure studies on the formation of phosphine modified cobalt carbonyl species were conducted using a sapphire NMR tube and by observing the ^{31}P nucleus. Experiments were designed specifically to determine the extent of modified hydride $HCo(CO)_3L$ formation for different ligands under standard catalyst pre-forming conditions (150 °C, 85 bar 2 : 1 syngas). The species observed corresponded well with previous high-pressure studies with PBu_3 and peak assignments were based on values reported in the literature.[24,25] The ^{31}P chemical shifts for the different Co phosphine species in solution are summarised in Table 4. The chemical shifts of the dimers were found at δ = 38–42 ppm and for the hydrides at δ = 26–30 ppm.

For all species two peaks, corresponding to the diastereomers of the ligand, were observed. The typical ^{31}P high pressure NMR spectrum showing the different cobalt phosphine species observed during the catalyst pre-forming reaction is depicted in Fig. 3. At 30 °C free ligand, the disproportionation salt $[Co(CO)_3L_2][Co(CO)_4]$ and dimer $[Co(CO)_3L]_2$ were evident in the spectrum. In accordance with the results for Lim-C_{18}, and predicted by molecular modelling, it was observed in all cases that one isomer coordinates preferentially to the metal centre. Upon heating to 90 °C, the salt resonances slowly decrease in intensity relative to the dimer, and a small amount of hydride $HCo(CO)_3L$ starts to form. At 120 °C the salt has disappeared completely and the hydride resonances have increased. After 2 hours at 150 °C a maximum amount of hydride is observed, this quantity is listed in Table 3 for the different ligands.

Hydride formation ranged between 22 and 33% with Lim-C_5 forming the most hydride. Fig. 1 clearly demonstrates that the HP-IR, HP-NMR and molecular modelling findings are complementary. As the percentage modified hydride increases, the ratio of modified to unmodified hydride increases and the calculated ligand coordination energy is less endothermic. These three techniques, though focussing on different aspects of the pre-catalytic species can be used to obtain qualitative information with regard to new ligands.

Kinetic measurements

As mentioned earlier the overall observed activity and selectivity of the catalytic mixture is a combined effect of hydroformylation through either the modified or unmodified cobalt systems. The unmodified Co-catalyst shows a higher reaction rate and chemioselectivity, while the modified catalyst is less reactive, but better regioselectivity towards the linear product is obtained. Thus a lower reaction rate and higher selectivity can be expected in catalyst systems where the ligand favours the formation of more modified species.

The influence of different ligands on the catalytic reactivity and selectivity in the hydroformylation of 1-dodecene was studied. The experiments were performed at 170 °C under 85 bar syngas (H_2 : CO ratio 2 : 1) with a cobalt concentration of 1000 ppm and a phosphine to cobalt ratio of 2 : 1 in all cases. The substrate was diluted to 50% (v/v) with a paraffinic solvent. Reactions were allowed to proceed until completion in order to preclude any differences in selectivity resulting from differences

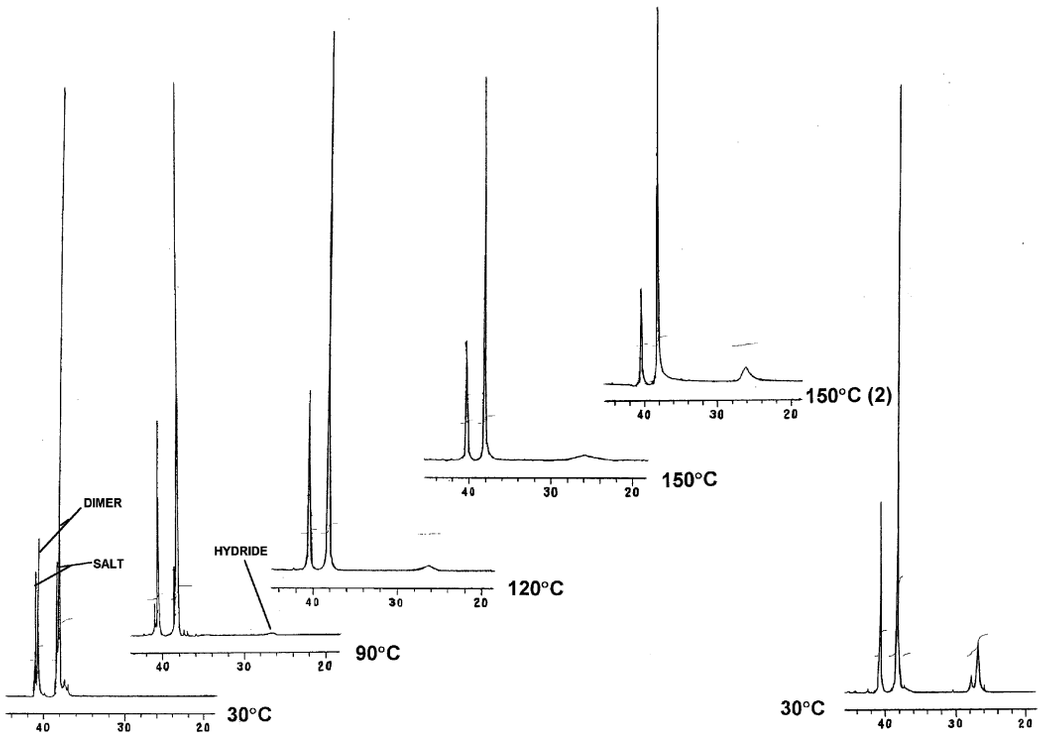

Fig. 3 $Co_2(CO)_8$ + Lim-C_{18}, Co : L = 1 : 2.5, 30–150 °C, 60–85 bar syngas.

Table 5 Summary of kinetic data

Ligand	n : iso	Linearity	Hydrogenation	k'
Lim-C_{18}	3.6	63.1	5.0	0.81
Lim-C_{10}	4.1	66.0	5.3	0.71
Lim-C_5	4.9	70.6	6.1	0.63
Lim-C_4	4.9	68.4	5.7	0.51
Lim-APh	3.0	58.7	5.8	1.1
Lim-ACN	2.6	54.8	5.6	1.6
Lim-ABE	3.4	58.8	5.1	0.97
Lim-EVE	3.4	61.3	5.1	0.91

in conversion. Pseudo k values were calculated from $-\ln(1 -$ conversion)/time plots generated from the mass of syngas consumed. The kinetic and selectivity results are presented in Table 5. Linearity ranges from 54 to 71% with Lim-ACN yielding the most branched product and Lim-C_5 the most linear product. The n : iso ratio (ratio of linear to 2-methyl branched alcohol) also followed the same trend with a ratio of 2.6 for Lim-ACN and 4.9 for Lim-C_5. According to expectations the rate decreases as the linearity increases with pseudo k values of 0.5 to 1.1. Hydrogenation of the alkene varied within a narrow band with 5–6% of the products consisting of dodecane.

Fig. 4 illustrates the relationship of the kinetic and selectivity trends to the modified to unmodified ratio as determined by HP-IR. It is clear that the modified to unmodified ratio correlates well with the observed reactivity and selectivity trends. A clear increase in the linearity, n : i and modified : unmodified and a subsequent decrease in the pseudo k value was observed as the alkyl chain length was reduced from C_{18} to C_{10} to C_5. The results for Lim-C_5 and Lim-C_4 were almost identical in all regards. For the ligands containing functionalised alkyl chains the effects induced are believed to be mainly electronic in nature with the more electronic deficient ligands corresponding to a lower modified : unmodified ratio.

Conclusion

It was shown that the family of bicyclic phosphines derived from (*R*)-(+)-limonene are exceptional ligands for the modified cobalt hydroformylation of 1-dodecene. The activity and selectivity is, to a large extent, governed by the equilibria between the modified and unmodified cobalt catalysts in solution with the different complexes identified using a combination of high pressure IR and NMR spectroscopic techniques. It was clearly illustrated that the modified cobalt catalyst is less reactive than the unmodified catalyst, but exhibits significantly improved regioselectivity towards the desired linear products.

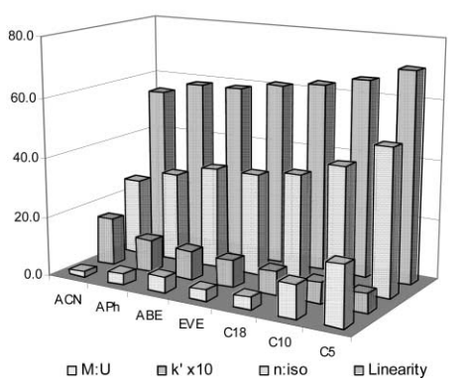

Fig. 4 Comparison of reactivity and selectivity trends with modified to unmodified ratio.

Acknowledgements

Financial support from Sasol Technology R&D is gratefully acknowledged as well as fruitful discussions with Prof. Mike Green, Manager Homogeneous Catalysis Research.

References

1 O. Roelen, *Ger. Pat.*, 949 548, 1938.
2 C. D. Frohning and C. W. Kohlpaintner, in *Applied Homogeneous Catalysis with Organometallic compounds*, eds. B. Cornils and W. A. Herrmann, VCH, Weinheim, 1996, vol. 1, p. 29.
3 L. H. Slaugh and R. D. Mullineaux, *J. Organomet. Chem.*, 1968, **13**, 469.
4 J. P. Collman, L. S. Hegedus, J. R. Norton and R. G. Finke, *Principles and Applications of Organotransition Metal Chemistry*, University Science Books, Mill Valley, California, 1987.

5 M. Beller, B. Cornils, C. D. Frohning and C. W. Kohlpainter, *J. Mol. Catal. A: Chem.*, 1995, **104**, 17.
6 F. Piacenti, M. Bianchi, E. Benedetti and P. Frediani, *J. Organomet. Chem.*, 1970, **23**, 257.
7 L. Rosi, A. Bini, P. Frediani, M. Bianchi and A. Salvini, *J. Mol. Catal. A: Chem.*, 1996, **112**, 367.
8 J. L. van Winkle, S. Lorenzo, R. C. Morris and R. F. Mason, *US Pat.*, 3420898, 1969.
9 J. P. Steynberg, K. Govender and P. J. Steynberg, *WO*, 2002014248, 2002.
10 B. Delley, *J.Chem. Phys.*, 1990, **92**, 508; B. Delley, *J. Phys. Chem.*, 1996, **100**, 6107; B. Delley, *J. Chem. Phys.*, 2000, **113**, 7756.
11 www.accelrys.com.
12 J. P. Perdew, *Phys. Rev. B*, 1986, **33**, 8822.
13 A. K. Rappé, C. J. Casewit, K. S. Colwell, W. A. Goddard and W. M. Skiff, *J. Am. Chem. Soc.*, 1992, **114**, 10024; A. K. Rappé, K. S. Colwell and C. J. Casewit, *Inorg. Chem.*, 1993, **32**, 3438; C. J. Casewit, K. S. Colwell and A. K. Rappé, *J. Am. Chem. Soc.*, 1992, **114**, 10035.
14 J. P. P. Stewart, *J. Comp. Chem.*, 1989, **10**, 209.
15 www.wavefun.com.
16 W. Rigby, R. Whyman and K. Wilding, *J. Phys. E*, 1970, **3**, 572.
17 D. C. Roe, *J. Magn. Res.*, 1985, **63**, 388; I. T. Horvath and J. M. Miller, *Chem. Rev.*, 1991, **91**, 1339.
18 A. Robertson, C. Bradaric, C. S. Frampton, J. McNulty and A. Capretta, *Tetrahedron Lett.*, 2001, **42**, 2609.
19 R. Ditchfield, *Mol. Phys.*, 1974, **27**, 789–807.
20 Gaussian 98, Revision A.11, M. J. Frisch, G. W. Trucks, H. B. Schlegel, G. E. Scuseria, M. A. Robb, J. R. Cheeseman, V. G. Zakrzewski, J. A. Montgomery, Jr., R. E. Stratmann, J. C. Burant, S. Dapprich, J. M. Millam, A. D. Daniels, K. N. Kudin, M. C. Strain, O. Farkas, J. Tomasi, V. Barone, M. Cossi, R. Cammi, B. Mennucci, C. Pomelli, C. Adamo, S. Clifford, J. Ochterski, G. A. Petersson, P. Y. Ayala, Q. Cui, K. Morokuma, P. Salvador, J. J. Dannenberg, D. K. Malick, A. D. Rabuck, K. Raghavachari, J. B. Foresman, J. Cioslowski, J. V. Ortiz, A. G. Baboul, B. B. Stefanov, G. Liu, A. Liashenko, P. Piskorz, I. Komaromi, R. Gomperts, R. L. Martin, D. J. Fox, T. Keith, M. A. Al-Laham, C. Y. Peng, A. Nanayakkara, M. Challacombe, P. M. W. Gill, B. Johnson, W. Chen, M. W. Wong, J. L. Andres, C. Gonzalez, M. Head-Gordon, E. S. Replogle and J. A. Pople, Gaussian, Inc., Pittsburgh, PA, 2001, rhf/6–311+g(2d,p) basis set.
21 C. J. Jameson, *Chem. Phys. Lett.*, 1990, **167**, 575–582; K. Eichele, R. E. Wasylishen, J. F. Corrigan, N. J. Taylor, A. J. Carty, K. W. Feindel and G. M. Bernard, *J. Am. Chem. Soc.*, 2002, **124**, 1541–1552.
22 D. J. Cole-Hamilton and S. Polas, unpublished work.
23 R. Whyman, *J. Organomet. Chem.*, 1974, **81**, 97.
24 K. W. Kramarz, R. J. Klingler, D. E. Fremgen and J. W. Rathke, *Catal. Today*, 1999, **49**, 339.
25 J. W. Rathke, K. W. Kramarz, R. J. Klinger, M. J. Chen, D. E. Fremgen and R. E. Gerald II, *Trends Organomet. Chem.*, 1999, **3**, 201.